PCCP

Comment on "Applicability of perturbed matrix method for charge transfer studies at bio/metallic interfaces: a case of azurin" by O. Kontkanen, D. Biriukov and Z. Futera, Phys. Chem. Chem. Phys., 2023, 25, 12479

Journal:	*Physical Chemistry Chemical Physics*
Manuscript ID	CP-CMT-07-2023-003178.R1
Article Type:	Comment
Date Submitted by the Author:	24-Aug-2023
Complete List of Authors:	Sarhangi, Setare ; Arizona State University, Physics Matyushov, Dmitry; Arizona State University, School of Molecular Sciences

PCCP

ARTICLE TYPE

Cite this: DOI: 00.0000/xxxxxxxxxx

Comment on "Applicability of perturbed matrix method for charge transfer studies at bio/metallic interfaces: a case of azurin" by O. Kontkanen, D. Biriukov and Z. Futera, Phys. Chem. Chem. Phys., 2023, 25, 12479

Setare Mostajabi Sarhangi[a] and Dmitry V. Matyushov*[a]

Received Date
Accepted Date

DOI: 00.0000/xxxxxxxxxx

Polarizability is a fundamental property of all molecular systems describing the deformation of the molecular electronic density in response to an applied electric field. The question of whether polarizability of the active site needs to be included in theories of enzymatic activity remains open. Hybrid quantum mechanical/molecular mechanical calculations are hampered by difficulties faced by many quantum-chemistry algorithms to provide sufficiently accurate estimates of the anisotropic second-rank tensor of molecular polarizability. In this Comment, we provide general theoretical arguments for the values of polarizability of the quantum region or a molecule which have to be reproduced by electronic structure calculations.

Transfer of electrons in biological systems is driven by fluctuations of the protein-water-membrane system to which electronic states of cofactors are coupled mostly by electrostatic interactions. The modulation of cofactors' electronic states is described by hybrid quantum mechanical/molecular mechanical methods as the first-order quantum-mechanical perturbation. It displaces the electronic energies by the energy of Coulomb interaction of the quantum-mechanical (QM) region with the surrounding medium, $E^C = \langle \Psi_0 | \hat{H}^C | \Psi_0 \rangle$, where Ψ_0 is the ground-state wave function of the QM site.[1] The first-order perturbation describes the interaction of the protein-water-membrane classical system with the unperturbed electronic density of the QM region. In contrast, the second-order QM perturbation in the Coulomb interaction Hamiltonian $\hat{H}^C$ incorporates polarization of the QM electronic cloud by the medium. This electronic polarization can be cast[2,3] in terms of the second-rank tensor of dipolar polarizability $\boldsymbol{\alpha}$ of the ground electronic state producing a shift of the electronic energy quadratic in the medium electric field $\mathbf{E}_s$ (second-order Stark effect[4])

$$E = E_0 + E^C - \frac{1}{2}\mathbf{E}_s \cdot \boldsymbol{\alpha} \cdot \mathbf{E}_s, \tag{1}$$

where E_0 is the vacuum energy. The vector $\mathbf{E}_s$ is the microscopic electric field of the medium at the redox site and no cavity-field correction employed in Stark spectroscopy[4,5] (see below) is required.

A series expansion of the electronic energy in the electric field is truncated at the second order in eqn (1). Terms of higher order can be obtained by diagonalizing the multipolar expansion Hamiltonian[6,7]

$$\hat{H} = \hat{H}_0 + \hat{H}^C - \hat{\boldsymbol{\mu}} \cdot \mathbf{E}_s, \tag{2}$$

where $\hat{\boldsymbol{\mu}}$ is the electronic dipole moment operator. The expansion beyond the second order involves corresponding hyperpolarizabilities[8] of the QM center accessible by nonlinear optical spectroscopy. The ground-state dipolar polarizability can be measured by depolarized light scattering,[9] and the polarizability change for a specific optical transition follows from Stark spectroscopy.[10] The quadratic expansion of eqn (1) is mostly consistent with the full matrix diagonalization[3] and is sufficient for the present discussion.

The progress of a half reduction reaction is monitored by the difference (energy gap) between the highest unoccupied molecular orbital of the oxidized state, to which electron is transferred, and the electrochemical potential of the metal electrode in the electrochemical cell, from which electron arrives. It is therefore sufficient to monitor the energy gap reaction coordinate[2,3,11]

$$X = \Delta E^C - \frac{1}{2}\mathbf{E}_s \cdot \Delta\boldsymbol{\alpha} \cdot \mathbf{E}_s, \tag{3}$$

where $\Delta\boldsymbol{\alpha} = \boldsymbol{\alpha}_{\rm Red} - \boldsymbol{\alpha}_{\rm Ox}$ is the difference of polarizability tensors in the reduced (Red) and oxidized (Ox) states of the QM region. The difference Coulomb energy $\Delta E^C = \sum_j \Delta q_j \phi_j$ is commonly calculated in terms of delocalization of the transferring electron over the atomic sites carrying the charges Δq_j ($\sum_j \Delta q_j = -e$) and interacting with the site electrostatic potentials ϕ_j. The atomic difference charges $\Delta q_j = q_j^{\rm Red} - q_j^{\rm Ox}$ follow from subtracting the atomic charges in Red (final) and Ox (initial) states.[12]

[a] School of Molecular Sciences and Department of Physics, Arizona State University, PO Box 871504, Tempe, Arizona 85287-1504, USA; E-mail: dmitrym@asu.edu

The first term in eqn (3), the change in the Coulomb energy, is what is typically monitored in computer simulations of protein electron transfer.[13,14] A question raised in a number of recent publications[2,3,12,15] is whether the second term in eqn (3) can affect the statistics of X. In other words, the question is whether the electrostatics of partial atomic charges Δq_j is sufficient to address the energetics of electronic transitions in proteins or, alternatively, the deformation (polarization) of the electronic density of the QM site by the surrounding medium has to be involved.

A recent paper[16] follows the previous report for the half reaction in cytochrome c (Cyt-c)[15] in asserting that polarizability is insignificant for the half reaction of reduction of azurin (in agreement with our calculations[12]). It is also claimed that a minimal number of excited states can be used to diagonalize the multipolar Hamiltonian in the perturbed matrix method[6,7] (eqn (2)) realizing the general strategy of the valence-bond formalism.[11] This Comment shows that the latter notion contradicts the established spectroscopy of azurin. A very large number of quantum states is required to describe the active site polarizability and its alteration with changing oxidation state. The question raised here is, therefore, twofold: (i) what is a physically motivated estimate of the active site polarizability? and (ii) is the the statistics of X significantly affected by the second term in eqn (3) involving the polarizability difference $\Delta\boldsymbol{\alpha}$?

The second-rank Cartesian polarizability tensor in each oxidation state can be estimated as the vacuum polarizability from the sequence of vacuum transition dipole vectors $\mathbf{m}_{0k}$ and energy gaps ΔE_{0k} between the ground and excited states

$$\boldsymbol{\alpha}_i = 2\sum_{k\neq 0}\frac{\mathbf{m}^i_{0k}\mathbf{m}^i_{k0}}{\Delta E^i_{0k}}, \tag{4}$$

where $i = \mathrm{Ox}, \mathrm{Red}$ specifies the oxidation state. The scalar isotropic polarizability is then given by the well-known sum-over-states expression[8,17] involving the oscillator strength (OS), f_{0k}, for the $0\rightarrow k$ transition

$$\alpha_{0i} = \tfrac{1}{3}\mathrm{Tr}[\boldsymbol{\alpha}_i] = 4\mathrm{Ry}^2 a_0^3\sum_{k>0}\frac{f^i_{0k}}{(\Delta E^i_{0k})^2}. \tag{5}$$

Here, $\mathrm{Ry} = e^2/(8\pi\varepsilon_0 a_0) \simeq 13.6$ eV is one Rydberg unit of energy and a_0 is the Bohr radius. The Thomas-Reiche-Kuhn sum rule[8,17] constrains the OSs by the number of electrons N_e in the QM region

$$\sum_k f_{0k} = \sum_{k\in b} f_{0k} + \sum_{k\in c} f_{0k} = N_e, \tag{6}$$

where the excitation spectrum is separated into the bound (b) and continuum (c) states.[8,18,19] If the first sum is associated with the number $N^b_e < N_e$ of electrons, one can construct the lower bound estimate for that portion of the isotropic polarizability. Given that the transition energies in the bound part of the spectrum fall below the ionization energy I_i, one obtains

$$\alpha^b_{0,i} > \alpha^{\min}_{0,i} = 4a_0^3 N^b_e(\mathrm{Ry}/I_i)^2 \tag{7}$$

for the isotropic polarizability α^b_{0i} assigned to transitions to the bound states. Likewise, the total polarizability is constrained from above as[18]

$$\alpha_{0i} < \alpha^b_{0i} + 4a_0^3 N^c_{e,i}(\mathrm{Ry}/I_i)^2 > 4a_0^3 N_{e,i}(\mathrm{Ry}/I_i)^2, \tag{8}$$

where $N^c_e = N_e - N^b_e$.

With $I_{\mathrm{Ox}} \simeq 4.75$ eV for azurin[20] and assuming $N^b_{e,\mathrm{Ox}} = N_{e,\mathrm{Ox}} = 333$ for the QM region in our calculations below, one obtains $\alpha^{\min}_{0,\mathrm{Ox}} \simeq 1619$ Å^3 in eqn (7). This value applies only to the QM region. It is still significantly higher than $\alpha^b_{0i} \simeq 15-16$ Å^3 from our calculations below, suggesting that the overwhelming portion of the integrated OS falls in the continuum excitation spectrum[19] (eqn (6)) and $N^b_e \ll N_e$. The continuum spectrum is not included in sum-over-states calculations and polarizabilities $\boldsymbol{\alpha}^b_i$ are likely to fall significantly below $\boldsymbol{\alpha}_i$[19] (see below). Eqn (5), when limited to the bound spectrum, is not reliable and alternative approaches need to be implemented. This note equally applies to full diagonalization of the Hamiltonian matrix in eqn (2) since it is also limited, in practical calculations, to transition dipoles calculated on bound states.

Adopting the second inequality in eqn (8) as a crude estimate for α_{0i}, one can evaluate the change in polarizability from adding one electron

$$\Delta\alpha_0 = \alpha_{0,\mathrm{Red}} - \alpha_{0,\mathrm{Ox}} \simeq 4a_0^3(\mathrm{Ry}/I_i)^2. \tag{9}$$

From this formula, $\Delta\alpha_0 = 4.9$ Å^3 for azurin. Assuming that the polarizability change is caused by a single transition with the transition dipole aligned along the x-axis of the molecular frame, the above estimate implies $\Delta\alpha_{xx} \simeq 3\Delta\alpha_0 \simeq 15$ Å^3. Eqn (9) leads to $\Delta\alpha_0$ independent of the number of electrons $N_{e,i}$. In contrast, the equation suggested in ref[21] anticipates $\Delta\alpha_0 \propto \alpha_{0i}$

$$\alpha_{0,\mathrm{Red}}\Delta E^{\mathrm{Red}}_{01} = \alpha_{0,\mathrm{Ox}}\Delta E^{\mathrm{Ox}}_{01}. \tag{10}$$

Given eqn (7), molecular polarizability scales with the number of electrons responsible for excitations to bound electronic states[22] and one expects that polarizability scales as $\propto a^3$ for a quantum site with the effective radius a. The scaling is however $\propto a^4$ for quantized states in semiconductor nanoparticles[23] since the energy gap between the electronic states in the denominator of eqn (5) scales as $\propto a^{-2}$ for spherical quantum dots (also note $\propto a^{3q}$, $q \simeq 1.4-1.6$[21] scaling for polyenes[21,22]). In the limiting case of conducting electrons, the polarizability of a metal sphere becomes[24] $\alpha_0 = a^3$. For organic molecules, it was argued that reproducing material refractive indexes through the Clausius-Mossotti equation requires correcting the metal sphere limit by a scaling factor $\zeta \simeq 0.3-0.5$[25]

$$\alpha_0 = \zeta a^3. \tag{11}$$

Given that refractive indexes of most materials fall in a narrow range of values, eqn (11) is expected to provide a reasonable estimate of the isotropic polarizability. The situation with polarizability anisotropy is less clear.

Anisotropy of the polarizability tensor is quantified by the

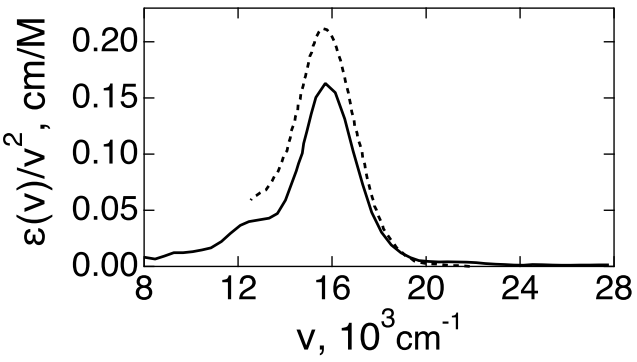

Fig. 1 $10^4 \times \varepsilon(\bar{\nu})/\bar{\nu}^2$ vs $\bar{\nu}$ for Ox azurin at 270 K and pH=7.[30] The dashed line refers to the azurin spectrum at 298 K and pH=5.[31]

scalar parameter[8,26]

$$\gamma^2 = \frac{1}{2}\left[3\mathrm{Tr}(\boldsymbol{\alpha}\cdot\boldsymbol{\alpha}) - \mathrm{Tr}(\boldsymbol{\alpha})^2\right]. \quad (12)$$

No constraints on the magnitude of γ have been established, but depolarized light scattering relates the relative anisotropy parameter[9] $\kappa = \gamma/(3\alpha_0)$ to the scattering depolarization ratio.

From experimental side, molecular polarizability can be related to the absorption spectrum by employing the relation between the imaginary part of the frequency-dependent polarizability $\alpha_0''(\omega)$ and the absorption cross section $\sigma_{\mathrm{abs}}(\omega)$[8,27]

$$\sigma_{\mathrm{abs}}(\omega) = \frac{4\pi\omega}{cn_D} f_c \alpha_0''(\omega), \quad (13)$$

where c is the speed of light in vacuum, n_D is the refractive index, and f_c is the cavity-field susceptibility connecting the field acting on a polarizable molecule with the Maxwell electric field in the medium.[4,28,29] By connecting the absorption cross section to the extinction coefficient[29] $\varepsilon_{\mathrm{abs}}(\omega)$ and using the Kramers-Krönig relation between the imaginary and real parts of the polarizability, one can obtain the isotropic polarizability in terms of the integrated absorption spectrum

$$\alpha_0 = \frac{10^3 \ln 10}{4\pi^3 N_A} \frac{3n_D^2}{n_D^2+2} \int_0^\infty \frac{d\bar{\nu}}{\bar{\nu}^2} \varepsilon_{\mathrm{abs}}(\bar{\nu}). \quad (14)$$

Here, the extinction coefficient is a function of the wave number $\bar{\nu}$ expressed in cm^{-1}, N_A is the Avogadro number, and the resulting polarizability carries the units of cm^3 given that the extinction coefficient is measured in $\mathrm{M}^{-1}\mathrm{cm}^{-1}$. The dispersion relation between the frequency and the wavenumber, $\nu = c\bar{\nu}/n_D$, produces the second power in the refractive index n_D and the Lorentz form[28,29] $f_c = (n_D^2+2)/3$ was adopted in eqn (14).

Applying eqn (14) to the absorption spectrum of Ox azurin (Fig. 1) results is $\alpha_0 \simeq 3$ Å^3. Integration of azurin's UV/VIS absorption spectrum contributes a small portion to the overall polarizability of the active site because of the limited frequency range. It is even a smaller fraction of the entire polarizability of azurin, $\alpha_{0i} \simeq 10^3$ Å^3, based on eqn (11). No information about polarizabillity anisotropy is allowed by absorption spectra.

Table 1 Extinction maxima ($10^3\mathrm{M}^{-1}\mathrm{cm}^{-1}$) of light absorption by protein cofactors and polarizability differences calculated from integrated absorption spectra (eqn (14)).

Cofactor	$\varepsilon_{\max}$	$\Delta\alpha_{xx}$, Å^3	Ref
Cu/azurin (Ox)	4	−9	[30]
GFP	60	−35[a]	[34]
Cytochrome *c* (Soret band, Red)	130	14	[37]
Bchl-a (Q_y band)	90	1	[35,38]
Fe_4S_4 (ferredoxin, 300 nm band)	46		[36]

[a]Taken between the excited and ground states of the GFP chromophore in contrast to two oxidation states in the cases of azurin, Bchl-a, and Cyt-c.

The intense optical transition in azurin's Ox state is enabled by the covalent character of the Cu-S(Cys-112) bond in the active site, and it is essentially absent in the Red state.[30–32] If one assumes that the difference in polarizabilities between Red and Ox states comes from this part of the absorption spectrum, one gets $\Delta\alpha_{xx} \simeq -9$ Å^3, where we have included the fact that polarizability due to absorption has only one diagonal component along the Cu-S(Cys-112) bond associated with the x-axis in the body frame. This value is of the same order of magnitude as those reported for other proteins. For instance, $\Delta\alpha_{0,\mathrm{ge}} = -35$ Å^3 was reported for the polarizability change between the ground (g) and excited (e) states in photoexcitation of green fluorescent chromophores (GFPs).[33] This higher value is consistent with a higher extinction coefficient of GFP[34] (Table 1). Extinction coefficient maxima for a number of cofactors commonly found in biological energy chains[35–38] are collected in Table 1.

The polarizability from UV/VIS absorption scales with the absorption intensity (eqn (14) and Table 1). Consistently, the application of eqn (14) to the spectra of bacteriochlorophyll-a[39] (BChl-a) and its reduced anion radical Bchl-a$^{\cdot-}$ (Fig. 2) results in higher polarizabilities: $\alpha_0(\mathrm{Bchl}) = 41.5$ Å^3 and $\alpha_0(\mathrm{Bchl}^{\cdot-}) = 41.9$ Å^3. Both numbers are somewhat below the polarizability $\simeq 60$ Å^3 estimated from eqn (11) and about twice lower than direct calculations: $\alpha_0(\mathrm{Bchl}) = 85.8$ and $\alpha_0(\mathrm{Bchl}^{\cdot-}) = 93.6$ Å^3 (B3LYP/6-311+g(d)), which are allowed in Gaussian 16[40] through fitting of the ground-state energy in the presence of the field[41] to the quadratic functionality in eqn (1).

Despite a noticeable distinction between absorption spectra of two oxidized forms (Figure 2), the resulting polarizabilities of BChl-a and Bchl-a$^{\cdot-}$ nearly cancel in the difference. In contrast, $\Delta\alpha_{0,\mathrm{ge}} = 18 \pm 3$ Å^3 was reported for the polarizability difference between the excited and ground states of Bchl-a by analyzing solvatochromism.[5] The resulting polarizability depends on pigment's chemical structure: the spectrum of BChl-a is compared to the spectrum of BChl-g[42] in Fig. 2. The polarizability from integrating the spectrum is higher for the latter, $\alpha_0(\mathrm{Bchl-g}) = 59$ Å^3.

The highest intensity among the cofactors listed in Table 1 belongs to the Soret absorption band of Cyt-c. Accordingly, integration of absorption spectra of Red and Ox states of Cyt-c[43] (Fig. 3) leads to $\alpha_{0,\mathrm{Red}} = 61.1$ Å^3 and $\alpha_{0,\mathrm{Ox}} = 56.6$ Å^3. Both numbers are significantly below $\alpha_{0,\mathrm{Red}} = 2180$ Å^3 estimated from eqn

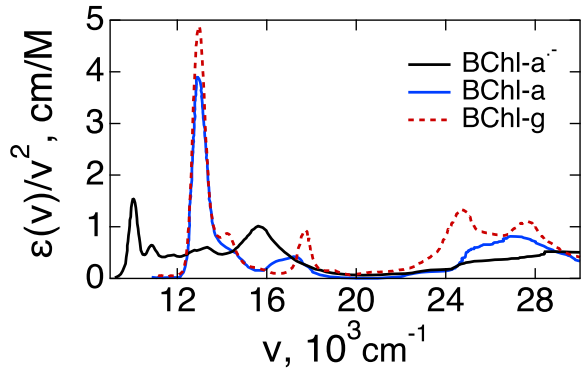

Fig. 2 $10^4 \times \varepsilon(\bar{\nu})/\bar{\nu}^2$ vs $\bar{\nu}$ for BChl-a and BChl-a$^{\cdot-}$ in dimethyl formamide at 298 K.[39] The red dashed line shows the spectrum of BChl-g[42] in benzene.

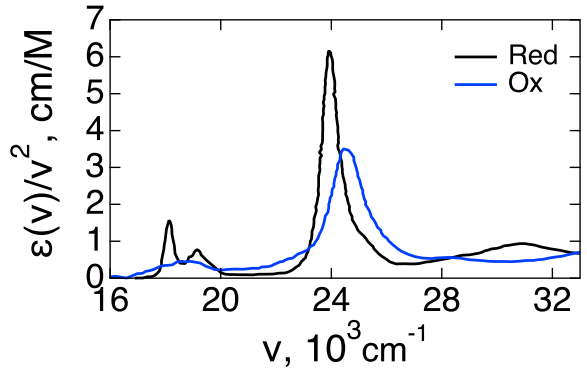

Fig. 3 $10^4 \times \varepsilon(\bar{\nu})/\bar{\nu}^2$ vs $\bar{\nu}$ for Red and Ox states of Cyt-c at 298 K.[43]

(11) with the Cyt-c radius $a \simeq 18.7$ Å.[44] This is expected given that absorption spectra represent polarizability of the QM region (heme and three ligating amino acids[2]) for which we obtained $\alpha_{0,\mathrm{Ox}} \simeq 95$ Å^3 and $\alpha_{0,\mathrm{Red}} \simeq 96$ Å^3 from eqn (11) with the effective radii calculated with Gaussian 16.[40] It appears that the UV/VIS spectrum captures about a half of the OS of the QM site in the case of Cyt-c, but this conclusion is of course affected by the subjective choice of the QM region. The polarizability difference between Red and Ox states becomes $\Delta\alpha_{xx} = 3\Delta\alpha_0 \simeq 14$ Å^3 for Cyt-c (Table 1) assuming that it is associated with a specific transition dipole oriented along the x-axis of the body frame.

Given that polarizability scales with the number of electrons, the bulk of it is not related to redox activity and should cancel out in the difference $\Delta\boldsymbol{\alpha} = \boldsymbol{\alpha}_{\mathrm{Red}} - \boldsymbol{\alpha}_{\mathrm{Ox}}$ (eqns (9) and (10)). To assess the typical values of the polarizability and its change with the altering oxidation state, one needs consistent calculations for a given molecular fragment sufficiently large to include the redox site. These calculations are listed in Table 2 for two oxidation states of the active site of azurin[12] composed of the Cu ion and five nearest amino acids ligating it.

The calculations listed in Table 2 apply either the sum-over-states eqn (5) or direct calculations of the polarizability in response to the applied electric field.[40] As expected, eqn (5)

Table 2 Isotropic, α_0, and anisotropic, γ, parts of the polarizability (Å^3) and the relative anisotropy parameter $\kappa = \gamma/(3\alpha_0)$ of Red and Ox states of azurin's active site calculated from different algorithms.

Calculation	α_0	γ	κ	eqn (11)[a]
Sum-over-states, eqn (4)				
ZINDO (Red)[b]	16.1	5.22	0.11	59 ± 3[c]
ZINDO (Ox)[b]	13.8	4.80	0.12	58 ± 5[c]
CIS/sdd (Red)[d]	15.7	11.6	0.25	50.8
CIS/sdd (Ox)[d]	13.1	8.64	0.22	66.7
Direct calculation with Gaussian 16				
B3LYP/6-31+g* (Red)	61.8	15.4	0.08	52 ± 1[c]
B3LYP/6-31+g* (Ox)	62.0	16.0	0.09	56 ± 5[c]
CIS/sdd[e] (Red)	48.8	11.8	0.08	50.8
CIS/sdd[e] (Ox)	47.9	12.2	0.08	66.7
CIS/6-31+g* (Red)	55.3	11.9	0.07	53 ± 3[c]
CIS/6-31+g* (Ox)	53.6	13.1	0.08	58 ± 5[c]
PBE/cc-pVTZ (Red)	64.7	18.3	0.09	
PBE/cc-pVTZ (Ox)	68.3	26.8	0.13	

[a]With $\zeta = 0.33$. [b]With 1000 excited states. [c]The volume of the QM site was calculated for a number of MD configurations to estimate the standard deviation. [d]With 500 excited states. [e]Calculations with a single frame including the effect of the protein medium gave very similar numbers of $\alpha_{0,\mathrm{Ox}} = 44.4$ and $\alpha_{0,\mathrm{Red}} = 47.0$ Å^3.

tends to underestimate the isotropic polarizability, but provides the anisotropy parameter $\kappa = \gamma/(3\alpha_0)$ in line with depolarized light scattering from small molecules.[45] The parameter κ is mostly unknown for proteins, except for $\kappa \simeq 0.5$ reported for Red Cyt-c.[46] The results of direct calculations employing the B3LYP/CIS/6-31+g* and PBE/cc-pVTZ protocols are most reliable[47,48] when compared to eqn (11), but both γ and $\Delta\alpha_0$ are too low in these calculations (cf. to Table 1).

The polarizability change $\Delta\boldsymbol{\alpha}$ produced by quantum calculations is insufficient to affect the energetics of half reduction reaction of azurin. In fact, finite-size corrections (omitted in refs[15,16]) related to the use of Ewald sums in the simulation protocol of a half reaction[49,50] exceed the effect of polarizability in this case.[12] The typical average electric field at the protein active site[12,51] is $E_s \simeq 0.2 - 0.4$ V/Å. Adopting $\Delta\alpha_{xx} \simeq 10$ Å^3 produces an energy shift of -0.03 eV in eqn (3), which is insufficient to substantially influence the energetics of electron transfer. A small difference polarizability $\Delta\alpha_0$ does not imply small polarizabilities of the active site in two oxidation states. In this regard, a recent assignment of $\alpha_{0i} \simeq 4$ Å^3 to the active site of azurin[16] is unphysical in not recognizing the linear scaling of polarizability with the number of electrons in the QM region. It is obviously inconsistent with the results of direct calculations presented in Table 2. Importantly, QM/MM formalisms applied to describe the deformation of the electronic density by electrostatic interactions with the classical region should be benchmarked to comply with eqn (11). The question of the difference polarizability to be used in modeling electron transfer is still not fully resolved since calculating the matrix $\Delta\boldsymbol{\alpha}$ invariably involves subtracting two large numbers to evaluate a relatively small difference.

Our calculations indicate that integrating UV/VIS absorption

spectra yields about a half of the value from eq (11) for the optically active Bchl and cytochrome's active site. The sum over states with parameters calculated from the bound part of the spectrum underestimates the overall molecular polarizability, but gives a reasonable estimate of the polarizability anisotropy. Isotropic polarizabilities based on the change of the ground-state energy in the electric field [40] (lower part in Table 2) fall sufficiently close to eqn (11).

Polarizabilities listed in Table 2 present vacuum calculations. Molecular polarizability fluctuates in the medium due to fluctuations of both the excitation energies ΔE_{0k} and the transition dipoles $\mathbf{m}_{0k}$ in eqn (4). Diagonalization of the Hamiltonian in eqn (2) ideally should account for both effects, but the restriction by the bound excitation spectrum makes this task unrealistic. Given this deficiency, the advantages of using the perturbed matrix method [6,7] (eqn (2)) are unclear. Eqn (3), supplemented with the polarizability matrix from high-level quantum-chemistry protocols, might provide a superior algorithm. Note that eqn (3) does not introduce additional computational load at the MD production stage. The analysis is performed on classical MD trajectories and requires only calculation of the electric field at the quantum site in addition to the standard calculation of the Coulomb interaction energy.

For the two-state problem, the transition moment in the medium $\mathbf{m}^s_{0i}$ is connected to the gas-phase transition dipole $\mathbf{m}_{0i}$ through the instantaneous medium energy gap ΔE^s according to the relation: [52] $\mathbf{m}^s_{0k}\Delta E^s_{0k} = \mathbf{m}_{0k}\Delta E_{0k}$. The medium polarizability for a single transition then scales as the third power of the ratio of gas-phase and medium energy gaps

$$\alpha^s_0 = \alpha_0(\Delta E_{0k}/\Delta E^s_{0k})^3. \quad (15)$$

In contrast, eqn (10) assumes no change to the transition dipole for the most significant lowest-energy excitation.

As a manifestation of the medium effect, the integrated OS was found to increase in polyenes when an external electric field was applied along the chain. [53] Likewise, changes of azurin absorption spectra with pH [31] (dashed line in Fig. 1) point to α_0 being affected by the local protein field. [4] As mentioned, most of OS falls into the continuum portion of the excitation spectrum and the medium effects can potentially focus OS into the discrete part of the spectrum to allow enhanced polarizability and light absorption.

In conclusion, polarizability is a fundamental property of all molecular systems describing the deformation of the molecular electronic density in response to an applied electric field. Frequency-dependent polarizability is related to light absorption and thus molecules with strong optical activity are also highly polarizable (eqn (13)). Many cofactors present in biological energy chains (porphyrins, hemes, copper sites in blue copper proteins) show significant optical activity and strong absorption bands in UV/VIS. This observation raises the question of whether high polarizability, coupled to a strong intraprotein electric field, is essential for the function of charge transport performed by these cofactors. Strong dependence of polarizabilities of conjugated molecules on conformation, [22] charge state, [21,22] and external electric field [4,53] was noted in the past and might be relevant to function performed by these cofactors.

The general theory of electron transfer between polarizable donor and acceptor [54] predicts lowering of the activation barrier compared to nonpolarizable systems. The evaluation of this barrier depression [2] is hampered by difficulties faced by many quantum-chemistry algorithms to provide sufficiently accurate estimates of the anisotropic second-rank tensor of molecular polarizability. The entire anisotropic polarizability matrix is essential given strong electric fields present inside proteins. [55–57] Computational formalisms should be benchmarked against the anticipated linear (or super-linear) scaling of polarizability with the number of electrons expressed by approximate relations in eqns (8) and (11). From the experimental side, second-order Stark effect provides the change of polarizability upon photoexcitation, [5,10,55] but polarizability changes associated with altering oxidation state are mostly unknown.

Acknowledgements

This research was supported by the National Science Foundation (CHE-2154465).

Notes and references

1 T. Kubař, M. Elstner and Q. Cui, *Ann. Rev. Biophys.*, 2023, **52**, 525–551.
2 M. Dinpajooh, D. R. Martin and D. V. Matyushov, *Sci. Rep.*, 2016, **6**, 28152.
3 D. R. Martin, M. Dinpajooh and D. V. Matyushov, *J. Phys. Chem. B*, 2019, **123**, 10691–1069.
4 S. G. Boxer, *J. Phys. Chem. B*, 2009, **113**, 2972–2983.
5 I. Renge and K. Mauring, *Spectrochimica Acta Part A: Mol. Biomol. Spectrosc.*, 2013-02-00, **102**, 301 – 313.
6 M. Aschi, R. Spezia, A. Di Nola and A. Amadei, *Chem. Phys. Lett.*, 2001, **344**, 374–380.
7 C. A. Bortolotti, A. Amadei, M. Aschi, M. Borsari, S. Corni, M. Sola and I. Daidone, *J. Am. Chem. Soc.*, 2012, **134**, 13670–13678.
8 K. D. Bonin and V. V. Kresin, *Electric-Dipole Polarizabilities of Atoms, Molecules, and Clusters*, World Scientific Publishing Co. Pte. Ltd., Singapore, 1997.
9 M. Kerker, *The Scattering of Light and Other Electromagnetic Radiation*, Academic Press, New York, 1969, vol. 16.
10 D. J. Lockhart and S. G. Boxer, *Proc. Natl. Acad. Sci. USA*, 1988, **85**, 107–111.
11 A. Warshel and R. M. Weiss, *J. Am. Chem. Soc.*, 1980, **102**, 6218–6226.
12 S. M. Sarhangi and D. V. Matyushov, *J. Phys. Chem. B*, 2022, **126**, 3000–3011.
13 D. N. LeBard and D. V. Matyushov, *Phys. Chem. Chem. Phys.*, 2010, **12**, 15335–15348.
14 J. Blumberger, *Chem. Rev.*, 2015, **115**, 11191–11238.
15 X. Jiang, Z. Futera and J. Blumberger, *J. Phys. Chem. B*, 2019, **123**, 7588–7598.
16 O. V. Kontkanen, D. Biriukov and Z. Futera, *Phys. Chem. Chem.*

Phys., 2023, **25**, 12479–12489.

17 G. C. Schatz and M. A. Ratner, *Quantum Mechanics in Chemistry*, Dover, New York, 1st edn., 2002.

18 T. M. Miller and B. Bederson, *Adv. Atom. Molec. Phys.*, 1978, **13**, 1–55.

19 L. Zheng, N. F. Polizzi, A. R. Dave, A. Migliore and D. N. Beratan, *J. Phys. Chem. A*, 2016, **120**, 1933–1943.

20 J. A. Fereiro, G. Porat, T. Bendikov, I. Pecht, M. Sheves and D. Cahen, *J. Am. Chem. Soc.*, 2018, **140**, 13317–13326.

21 S. M. Smith, A. N. Markevitch, D. A. Romanov, X. Li, R. J. Levis and H. B. Schlegel, *J. Phys. Chem. A*, 2004, **108**, 11063–11072.

22 C. P. de Melo and R. Silbey, *J. Chem. Phys.*, 1988, **88**, 2558–2566.

23 F. Wang, J. Shan, M. A. Islam, I. P. Herman, M. Bonn and T. F. Heinz, *Nature Materials*, 2006, **5**, 861–864.

24 L. D. Landau and E. M. Lifshitz, *Electrodynamics of Continuous Media*, Pergamon, Oxford, 1984.

25 P. Suppan, *Chem. Phys. Lett.*, 1983, **94**, 272–275.

26 C. G. Gray and K. E. Gubbins, *Theory of Molecular Liquids*, Clarendon Press, Oxford, 1984, vol. 1: Fundamentals.

27 G. D. Mahan and K. R. Subbaswamy, *Local Density Theory of Polarizability*, Plenum Press, New York, 1990.

28 C. J. F. Böttcher, *Theory of Electric Polarization, Vol. 1: Dielectrics in Static Fields*, Elsevier, Amsterdam, 1973.

29 D. V. Matyushov, *Manual for Theoretical Chemistry*, World Scientific Publishing Co. Pte. Ltd., New Jersey, 2021.

30 E. I. Solomon, J. W. Hare, D. M. Dooley, J. H. Dawson, P. J. Stephens and H. B. Gray, *J. Am. Chem. Soc.*, 1980, **102**, 168–178.

31 K. M. Clark, Y. Yu, N. M. Marshall, N. A. Sieracki, M. J. Nilges, N. J. Blackburn, W. A. van der Donk and Y. Lu, *J. Am. Chem. Soc.*, 2010, **132**, 10093–10101.

32 E. I. Solomon, *Inorg. Chem.*, 2006, **45**, 8012–8025.

33 M. Drobizhev, P. R. Callis, R. Nifosì, G. Wicks, C. Stoltzfus, L. Barnett, T. E. Hughes, P. Sullivan and A. Rebane, *Sci. Rep.*, 2015, **5**, 13223.

34 S. Mukherjee and R. Jimenez, *J. Phy. Chem. B*, 2022, **126**, 735–750.

35 R. E. Blankenship, *Molecular Mechanisms of Photosynthesis*, Blackwell Science, Williston, VT, 2003.

36 E. C. Hatchikian, M. Bruschi, N. Forget and M. Scandellari, *Biochem. Biophys. Res. Comm.*, 1982, **109**, 1316–1323.

37 R. E. Dickerson and R. Timkovich, in *Cytochromes c*, ed. P. D. Boyer, Academic Press, 1975, vol. 11, pp. 397–547.

38 M. Taniguchi and J. S. Lindsey, *Photochem. Photobiol.*, 2021, **97**, 136–165.

39 J. Fajer, D. C. Borg, A. Forman, D. Dolphin and R. H. Felton, *J. Am. Chem. Soc.*, 1973, **95**, 2739–2741.

40 M. J. Frisch, G. W. Trucks, H. B. Schlegel, G. E. Scuseria, M. A. Robb, J. R. Cheeseman, G. Scalmani, V. Barone, G. A. Petersson, H. Nakatsuji, X. Li, M. Caricato, A. V. Marenich, J. Bloino, B. G. Janesko, R. Gomperts, B. Mennucci, H. P. Hratchian, J. V. Ortiz, A. F. Izmaylov, J. L. Sonnenberg, D. Williams-Young, F. Ding, F. Lipparini, F. Egidi, J. Goings, B. Peng, A. Petrone, T. Henderson, D. Ranasinghe, V. G. Zakrzewski, J. Gao, N. Rega, G. Zheng, W. Liang, M. Hada, M. Ehara, K. Toyota, R. Fukuda, J. Hasegawa, M. Ishida, T. Nakajima, Y. Honda, O. Kitao, H. Nakai, T. Vreven, K. Throssell, J. A. Montgomery, Jr., J. E. Peralta, F. Ogliaro, M. J. Bearpark, J. J. Heyd, E. N. Brothers, K. N. Kudin, V. N. Staroverov, T. A. Keith, R. Kobayashi, J. Normand, K. Raghavachari, A. P. Rendell, J. C. Burant, S. S. Iyengar, J. Tomasi, M. Cossi, J. M. Millam, M. Klene, C. Adamo, R. Cammi, J. W. Ochterski, R. L. Martin, K. Morokuma, O. Farkas, J. B. Foresman and D. J. Fox, *Gaussian16 Revision C.01*, 2016, Gaussian Inc. Wallingford CT.

41 D. Hait and M. Head-Gordon, *Phys. Chem. Chem. Phys.*, 2018, **20**, 19800–19810.

42 *Chlorophylls and Bacteriochlorophylls. Biochemistry, Biophysics, Functions and Applications*, ed. B. Grimm, R. J. Porra, W. Rüdiger and H. Scheer, Springer Netherlands, 2006, vol. 25 of Advances in Photosynthesis and Respiration Series, ch. 6, pp. 79–94.

43 D. Heitmann and O. Einsle, *Biochemistry*, 2005, **44**, 12411–12419.

44 M. Heyden and D. V. Matyushov, *J. Phys. Chem. B*, 2020, **124**, 11634–11647.

45 F. Pabst and T. Blochowicz, *J. Chem. Phys.*, 2022, **157**, 244501.

46 L. Reinisch, K. T. Schomacker and P. M. Champion, *J. Chem. Phys.*, 1987, **87**, 150–158.

47 A. L. Hickey and C. N. Rowley, *J. Phys. Chem. A*, 2014, **118**, 3678–3687.

48 O. Feighan, F. R. Manby and S. Bourne-Worster, *J. Chem. Phys.*, 2023, **158**, 024107.

49 R. Ayala and M. Sprik, *J. Phys. Chem. B*, 2008, **112**, 257–269.

50 D. V. Matyushov, *J. Chem. Phys.*, 2021, **155**, 114110.

51 P. Geissinger, B. E. Kohler and J. C. Woehl, *Synthetic Metals*, 1997, **84**, 937–938.

52 D. V. Matyushov and M. D. Newton, *J. Phys. Chem. B*, 2019, **123**, 6564–6578.

53 L. Zheng, A. Migliore and D. N. Beratan, *J. Phys. Chem. B*, 2020, **124**, 6376–6388.

54 D. V. Matyushov and G. A. Voth, *J. Chem. Phys.*, 2000, **113**, 5413–5424.

55 S. D. Fried and S. G. Boxer, *Acc. Chem. Res.*, 2015, **48**, 998–1006.

56 D. R. Martin and D. V. Matyushov, *J. Phys. Chem. Lett.*, 2020, **11**, 5932–5937.

57 D. Bím and A. N. Alexandrova, *Chem. Sci.*, 2021, **12**, 11406–11413.